

# Baryons from quarks in curved space and deconfinement

M. Kirchbach and C. B. Compean,  
Instituto de Física, Universidad Autónoma de San Luis Potosí,  
Av. Manuel Nava 6, Zona Universitaria,  
S.L.P. 78290, México

**Abstract:** Detailed account is given of the fact that the Cornell potential predicted by Lattice QCD and its exactly solvable trigonometric extension recently reported by us can be viewed as the respective approximate and exact counterparts on a curved space to an  $1/r$  flat space potential. The “curved” potential describes a confinement phenomenon as it is of infinite depth and has only bound states. It furthermore has the remarkable property of preserving both the  $SO(4)$  and  $SO(2, 1)$  symmetries characterizing the ordinary  $1/r$  potential. We first make the case that this particular geometric vision on confinement provides a remarkably adequate description of both nucleon and  $\Delta$  spectra and the proton mean square charge radius as well, and suggests an intriguing venue toward quark deconfinement as a shut-down of the curvature considered as temperature dependent. Next we observe that the  $SO(2, 1)$  symmetry of the “curved” potential allows to place it within the context of  $AdS_5/CFT$  correspondence and to establish in this manner the algebraic link of the latter to QCD potentiology.

“...there will be no contradiction in our mind if we assume that some natural forces are governed by one special geometry, while other forces by another.”

N. I. Lobachevsky

## 1 Introduction

One of the major achievements of contemporary physics concerns the insight on the non-trivial geometry of the Universe. According to general theory of relativity, the space is curved by the presence of mass, a well established concept which was successful in explaining the precession of the orbit of Mercury and the bending of light in the vicinity of the Sun. Various geometries have been under consideration ever since in gravity, the closed Einstein’s universe of constant positive and the open one of Lobachevsky of constant negative curvature being among the most prominent versions (see [1],[2] for contemporary treatises). On long term, the ideas of general relativity exercised a profound impact on the development of quantum physics. On the one hand, they led to the geometric interpretation of gauge theories (see [3] for a pedagogic presentation) and on the other, they triggered progress in merging external space-time with internal gauge degrees of freedom which culminated in superstring and supergravity theories.

Perhaps nothing expresses relevance of the above movements better but the surprisingly modernly sounding statement made by Lobachevsky approximately 200 years ago (taken from ref. [4]) which we used as motto to the present article. Indeed, the geometric view on both space time and gauge theories suggests that some of the fundamental physics phenomena might be related to curvature, an obvious candidate being the color confinement phenomenon.

The idea that quark confinement might reflect some kind of curvature has been pioneered by Salam and Strathdee [5] who found a black-hole solution of Einstein’s equation approximate to the anti-de Sitter  $AdS_5$  geometry which describes strongly interacting tensor fields confined in a micro-universe of a radius fixed by the negative cosmological constant and which they interpreted as a

sort of hadron bag. In this manner, particles have been described within gravitational context as strongly curved universes, an idea pursued by several authors within various contexts [6]. Among the achievements of this idea we count (i) the explanation of the flavor independent level spacings of the radial excitation spectra of mesons following from the local isomorphism between the anti-de Sitter group  $SO(3,2)$  and  $Sp(4,R)$ , the symmetry group of the two-dimensional harmonic oscillator, (ii) the understanding of quark confinement as divergence of the bag radius due to its thermal dependence leading to space flattening [7]. Some of the constituent quark models, such as the MIT bag, the “Chashire cat” or the Skyrme models have been interpreted (roughly speaking) as black holes of anti-de Sitter geometry.

From the outgoing 90ies onward, the idea of the geometric confinement and the study of AdS space-time manifolds experienced a strong push, now from the new perspective of the  $AdS_5/CFT$  correspondence according to which a maximal supersymmetric Yang-Mills conformal field theory (CFT) in four dimensional Minkowski space is equivalent to a type IIB closed superstring theory in ten dimensions described by the product manifold  $AdS_5 \times S^5$  [8]. More recently, the correspondence between string theory in ten dimensional anti-de Sitter space and  $SO(4,2)$  invariant conformal Yang-Mills theories has been adapted in [9] to the description of hadron properties.

Parallel to the above achievements, significant progress in understanding hadron properties has been reached independently through the elaboration of the connection between the QCD Lagrangian and the potential models as deduced within the framework of effective field theories and especially through the non-perturbative methods such as lattice simulations [10],[11], the most prominent outcome being the linear plus Coulomb confinement potential [12], [13]. The potentials derived from the QCD Lagrangian have been most successful in the description of heavy quarkonia and heavy baryon properties [14]. Although the Cornell potential has found applications also in nucleon and  $\Delta$  quark models [15], the provided level of quality in the description in the non-strange sector stays below the one reached for the heavy flavor sector. This behavior reflects insufficiency of the one gluon exchange (giving rise to the Coulomb-like term) and of the flux-tube interaction (associated with the linear part) to account for the complexity of the dynamics of three light quarks. Various improvements have been under consideration in the literature such as screening effects in combination with spin-spin forces (see [16] and reference’s therein).

Very recently, the Cornell potential has been updated through its extension toward an exactly solvable (in the sense of the Schrödinger equation, or, the Klein-Gordon equation with equal scalar and vector potentials) trigonometric quark confinement potential [17]. The latter potential, which has the property of interpolating between a Coulomb-like potential and the infinite well while passing through a region of linear growth, was shown to provide a remarkably good description of the spectra of the non-strange baryons, the nucleon and the  $\Delta$ , considered as quark-diquark systems, and of the proton charge radius as well. Especially the observed hydrogen-like degeneracy patterns in the above spectra in the non-trivial combination with the non-hydrogen like (because increasing instead of decreasing) level spacings found a stringent explanation in terms of the  $SO(4)$  symmetry of the trigonometric potential.

The main goal of the present work is to draw attention to the fact that similarly to the Coulomb-potential, the trigonometrically extended Cornell (TEC) potential, possesses next to  $SO(4)$  also  $SO(2,1)$  symmetry as manifest through the possibility to cast its spectrum as well in terms of  $SO(4)$  as in terms of  $SO(2,1)$  Casimirs. The  $SO(2,1)$  versus  $SO(4)$  symmetry correspondence allows to place the TEC potential within the context of  $AdS_5$  versus  $CFT$  correspondence and in this manner to link the algebraic aspects of  $AdS_5/CFT$  to QCD potentiology [10]. Such is possible because while  $SO(2,1)$  appears in one of the possible  $AdS_5$  reduction chains [18], namely,

$$SO(3,2) \subset SO(2,2) \subset \underline{SO(2,1)} \subset SO(2), \quad (1)$$

$SO(4)$  appears within the reduction chain associated with  $CFT$ ,

$$SO(4,2) \subset SO(4,1) \subset \underline{SO(4)} \subset SO(3) \subset SO(2). \quad (2)$$

It is important to be aware of the fact that the algebraic  $AdS_5/CFT$  criteria alone are not sufficient to fix uniquely the potential. One has to complement them by the requirement on compatibility with the QCD Lagrangian too, a condition which imposes severe restrictions on the allowed potential shapes.

Our next point is that algebraically the  $AdS_5/CFT$  correspondence translates into  $SO(2,1)/SO(4)$  symmetry correspondence of the potential and that it is the trigonometrically extended Cornell potential, treated as quark-diquark potential, the one that meets best both the  $AdS_5/CFT$  and QCD criteria and provides the link between them. Predicted degeneracy patterns and level splitting are such that none of the observed  $N$  states drops out of the corresponding systematics which also applies equally well to the  $\Delta$  spectra (except accommodation of the hybrid  $\Delta(1600)$ ). The scenario provides a remarkable description of the proton charge electric form-factor too and moreover implies a deconfinement mechanism as a shut-down of the curvature considered as temperature dependent.

The group symmetries under discussion appear within the context of a Schrödinger equation written in different variables. Specifically for the case of the hydrogen atom these different variables have been extensively studied and are well known. The  $SO(4)$  appears as symmetry of the standard radial part,  $R(r)$ , of the Schrödinger wave function, with  $r$  standing as usual for the radial distance, while  $SO(2,1)$  is the symmetry of same equation when transformed to  $r = y^2$  and  $R(r) = y^{-\frac{3}{2}}Y(y)$  variables [19],[20]. Obviously, in the specific case under consideration, both symmetries are physically indistinguishable because they both lead to same physical observables such as spectrum and transition probabilities. Preferring the one over the other as mathematical tool in hydrogen description is a pure matter of convenience and giving preference to  $SO(4)$  is only more popular. The Coulomb potential is an example that matches algebraically  $AdS_5/CFT$  correspondence but is at odds with the non-perturbative aspects of QCD dynamics.

The TEC case of major interest in this work presents itself bit more involved. While the Schrödinger equation giving rise to the  $SO(4)$  symmetric spectrum is well studied and well understood in terms of a potential satisfying the Laplace-Beltrami equation on the three dimensional (3D) hypersphere,  $S_R^3$ , of constant radius,  $R$ , i.e. on a curved space of a constant positive curvature, knowledge on the differential realization of the  $SO(2,1)$  symmetry on a hyperbolic space is quite scarce indeed (see next section). Filling this technical gap should certainly be beyond the scope of the present study which main focus are spectroscopic observables. However, a strong though indirect hint on the relevance of  $SO(2,1)$  for the TEC problem is provided by the possibility to recast its spectrum in terms of  $SO(2,1)$  Casimir eigenvalues (admittedly, for limited values of the strength parameter [21]). In other words, at least for some particular values of the strength parameters a manifest coordinate transformation of the Schrödinger equation with the TEC potential from a four-dimensional Euclidean to a three dimensional hyperbolic geometry is likely to exist. Of course, unless such a transformation has not been explicitly constructed, no algebraic formalization of a possible indistinguishability between the respective  $SO(4)$  and  $SO(2,1)$  symmetries can be claimed. Rather, one has to make a side by side comparison of the predictions of both schemes with the aim of proving their proximity, a subject treated in Section 4 below.

Finally, besides viewing  $SO(4)$  as part of  $CFT$ , it can also be embedded within an (admittedly, Euclidean) anti-de Sitter space [22],

$$-x_5^2 + x_0^2 + x_1^2 + x_2^2 + x_3^2 = -l^2, \quad (3)$$

where the  $x_i$  with  $i = 1, 2, 3$  are the usual Cartesian coordinates in standard position space,  $x_5$  and  $x_0$  are the two time-like dimensions, from which the second has been “Wick rotated”, and  $-1/l^2$  is the negative curvature. This additional insight provides, in our view, a further legitimization for accepting, without too much a loss of generality, the hypersphere  $x_0^2 + x_1^2 + x_2^2 + x_3^2 = R^2$  as a mathematical tool in the description of quark confinement as infinite potential barrier, a venue that takes directly to the trigonometric extension of the Cornell potential. In taking this path, however, one should treat the positive curvature,  $\kappa = 1/R^2$ , introduced in that manner, with

some care and detain from equipping it with too deep a physical meaning. Rather it should be viewed as a second phenomenological parameter next to the potential strength which so far stays uncorrelated to the physical cosmological constant,  $\lambda = -1/l^2$ . We shall show that while spectra and charge form factors remain by and large insensitive to this parameter, it provides a valuable phenomenological tool for deconfinement description in the spirit of ref. [7].

The outline of the paper is as follows. The next section is a historic survey on the quantum Kepler problem in a space of constant positive curvature, the 3D hypersphere,  $S_R^3$ , a survey that begins with early work by Schrödinger [23]. A detailed account is given of the fact that the harmonic potential on  $S_R^3$ , i.e. the one that satisfies the four-dimensional angular Laplace-Beltrami equation, takes the form of the trigonometric confinement potential  $-2b \cot \chi + l(l+1) \csc^2 \chi$  (with  $\chi$  standing for the second polar angle). Depending on the  $\chi$  parametrization in terms of coordinates in ordinary position space, a variety of potentials can be created. Examples are the the exactly solvable trigonometric extension of the Cornell quark confinement potential, around which the present work is centered, and which corresponds to  $\chi = r\sqrt{\kappa}\pi$  where  $r$  is the absolute value of the radius vector, and  $\kappa$  is the curvature of the hypersphere. Another version would be a gradient dependent confinement potential for particles with position and curvature dependent mass as needed for the purposes of quantum dots. We attend also this more subtle version because of its possible relevance for the description of the evolution of finite valence to vanishing parton quark masses. These two examples are presented in section 3. Section 4 focuses on the application of the trigonometric extension of the Cornell potential to the spectra of the nucleon and the  $\Delta$  considered as quark-diquark systems. It further contains the description of same spectra within the  $SO(2,1)$  symmetric version of same potential thus revealing its link to the algebraic aspects of the  $AdS_5/CFT$  scenario. The section ends with a calculation of the mean square proton charge radius. Section 5 presents the property of energy spectrum and wave functions of the TEC problem to collapse upon curvature shut-down (i.e. in the large  $R$  limit) to the bound and scattering states of ordinary flat-space  $1/r$  potential, a peculiarity that we employ (in parallel to Takagi's work [7] mentioned above) to interpret deconfinement as flattening of space due to a thermal dependence of the curvature parameter. The paper closes with brief summary and outlooks.

## 2 Harmonic potential on $S_R^3$ : The survey

The first to have considered the Coulomb potential on a curved space has been Schrödinger who solved in [23] the quantum mechanical Coulomb problem in the cosmological context of Einstein's universe, i.e. on the three dimensional (3D) hypersphere,  $S_R^3$ , of a constant radius  $R$ . Schrödinger's prime result, the presence of curvature provokes that the orbiting particle appears confined within a trigonometric potential of infinite depth and the hydrogen spectrum shows only bound states. An especially interesting observation was that the  $O(4)$  degeneracy of the levels observed in the flat space  $H$  atom spectrum was preserved by the curved space spectrum too in the sense that also there the levels could be labeled by the standard atomic indices  $n$ ,  $l$ , and  $m$ , and the energy depended on  $n$  alone. However, contrary to flat space, no explicit form of  $O(4)$  generators could be immediately exhibited. Although Higgs [24] and Leemon [25] succeeded in constructing on  $S_R^3$  the respective analogue to the Runge-Lenz vector in flat space, no way was found to incorporate it into the  $O(4)$  group algebra. Instead, Barut and collaborators [26] designed a version of the potential as a differential  $su(1,1)$  Casimir operator in allowing one of the potential parameters to depend on the principal quantum number in a very particular way. However, this version, strictly speaking, does not share the original  $SO(4)$  degeneracy patterns and is not of interest to the present study.

Perhaps because Schrödinger used the curved space Coulomb problem as an example for exact solubility of his celebrated equation by means of the factorization technique, it became more popular in that very context than in any other giving rise to the field of physics known as supersymmetric quantum mechanics (SUSYQM), a historical development mainly triggered by subsequent extensive work by Infeld and collaborators [27] and later on by Witten [28].

Nonetheless, also the geometric aspect of Schrödinger's work was independently picked up by

several researchers and placed within various contexts. The idea of using such “curved” potentials gradually breached into several areas of quantum physics from atomic [29] to the utmost modern nano-tubes physics [30], and sophisticated non-linear  $W$  algebra symmetries [31] viable in string theories. Bessis et al. [29] applied it to fine structure analysis of atomic spectra, Ballesteros and Herraz [32] considered it within the context of quantum algebras, while Roy and Roychoudhuri formulated SUSYQM in a 3D curved space [33]. Also the Russian school provided notable contributions especially regarding the mathematical aspects of the solutions [34].

It is worth noticing that also the harmonic oscillator (HO) potential has been considered on  $S_R^3$  in [24], [36]. Finally, both the Coulomb and the HO problems have been also solved in spaces with a negative constant curvature (Lobachevsky geometry) in the second reference [27], and in [37], [38], to mention only few representative examples of such studies (see also ref. [2] for a recent up-date).

The current section is a historic survey on the quantum Kepler problem in a space of constant positive curvature, the 3D hypersphere,  $S_R^3$ . It contains a detailed account of the fact that the harmonic potential on  $S_R^3$ , i.e. the one that satisfies the four-dimensional Laplace-Beltrami equation, takes the form of the trigonometric confinement potential  $-2b \cot \chi + l(l+1) \csc^2 \chi$  (with  $\chi$  standing for the second polar angle).

## 2.1 $S_R^3$ parametrization and curved space Coulomb-like potential

From now onward the usual three dimensional flat Euclidean space,  $E_3$ , will be embedded in the four dimensional Euclidean space,  $E_4$ . A set of generalized Cartesian coordinates,  $\{x_1, x_2, x_3, x_4\}$ , in  $E_4$  chosen to parametrize a three-dimensional spherical surface there, has to satisfy the condition,

$$s^2 = x_1^2 + x_2^2 + x_3^2 + x_4^2, \quad \kappa = \frac{1}{s^2}, \quad 0 < s < \infty, \quad (4)$$

where  $s$  is the hyper-radius, and  $\kappa$  the corresponding curvature. A Coulomb-like potential in any  $E_n$  space is defined from the requirement to be harmonic, i.e. to obey the respective  $n$ -dimensional Laplace-Beltrami equation in charge free spaces. Specifically in  $E_4$  such a potential, call it  $v(\bar{x})$ , where  $\bar{x}$  denotes the radius vector of a generic point on the hypersphere, is most easily found in Cartesian coordinates

$$\square v(\bar{x}) = \sum_{i=1}^{i=4} \frac{\partial^2}{\partial x_i^2} v(\bar{x}) = 0, \quad (5)$$

and reads

$$v(\bar{x}) = c \frac{x_4}{\bar{r}}, \quad \bar{r} = \sqrt{x_1^2 + x_2^2 + x_3^2}. \quad (6)$$

Here,  $\bar{r}$  is the length of the radius vector in the  $E_3$  subspace of  $E_4$ ,  $c$  is a constant, and use has been made of the fact that the  $1/\bar{r}$  potential is harmonic in  $E_3$  as it satisfies there the three-dimensional Laplace equation,  $\vec{\nabla}^2(1/\bar{r}) = 0$ . Changing now to hyperspherical coordinates,  $\Omega = \{\chi, \theta, \varphi\}$ , results in

$$\begin{aligned} x_1 &= \bar{r} \sin \theta \cos \varphi, & x_2 &= \bar{r} \sin \theta \sin \varphi, \\ x_3 &= \bar{r} \cos \theta, & x_4 &= s \cos \chi, \\ \bar{r} &= s \sin \chi, \quad 0 \leq \chi \leq \pi, & 0 \leq \theta \leq \pi, \quad 0 \leq \varphi \leq 2\pi. \end{aligned} \quad (7)$$

In terms of  $\chi$ , the “curved”  $1/\bar{r}$  potential is read off from eq. (7) as the following trigonometric potential,

$$v\left(\frac{x_4}{\bar{r}}\right) \equiv v(\chi) = c \cot \chi. \quad (8)$$

This is a very interesting situation in so far as in  $E_4$  the rôle of the radial coordinate of infinite range in ordinary flat space,  $0 < \bar{r} < \infty$ , has been taken by the angular variable,  $\chi$ , of finite range. In other words, while the harmonic potential in  $E_3$  is a central one, in  $E_4$  it is non-central. Moreover,

the inverse distance potential of finite depth in  $E_3$  is converted to an infinite barrier and therefore to a confinement potential in the higher dimensional  $E_4$  space, a property of fundamental importance throughout the paper.

## 2.2 Schrödinger's geometric quantum scheme

This section contains a detailed account of Schrödinger's treatment [23] of the quantum mechanical Coulomb problem within Einstein's cosmological concept, i.e. on the three dimensional sphere of constant radius,  $S_R^3$ . For this purpose, Schrödinger had to solve his celebrated equation in  $E_4$ . The equation is not only especially simple to solve on the hypersphere of constant radius,  $s = R = \text{const}$ , where it is purely angular, but it is also there where it acquires a special physical importance, to be revealed below.

When written in the hyper-spherical coordinates, it takes the following form,

$$\left(-\kappa \frac{\hbar^2}{2\mu} \hat{\square} + c \cot \chi\right) \Psi(\chi, \theta, \varphi, \kappa) = E(\kappa) \Psi(\chi, \theta, \varphi, \kappa), \quad \kappa = \frac{1}{R^2} = \text{const}, \quad (9)$$

where  $\hat{\square}$  denotes the angular (hyperspherical) part of the  $E_4$  Laplace-Beltrami operator. Here, and without loss of generality, the potential strength has been kept unspecified so far and denoted by the constant  $c$ . Using the well known representation of  $\hat{\square}$ ,

$$\begin{aligned} \hat{\square} &= \left[ \frac{1}{\sin^2 \chi} \frac{\partial}{\partial \chi} \sin^2 \chi \frac{\partial}{\partial \chi} - \frac{L^2}{\sin^2 \chi} \right], \\ L^2 &= - \left[ \frac{1}{\sin \theta} \frac{\partial}{\partial \theta} \sin \theta \frac{\partial}{\partial \theta} + \frac{1}{\sin^2 \theta} \frac{\partial^2}{\partial \varphi^2} \right], \end{aligned} \quad (10)$$

where  $L^2$  is the standard three dimensional orbital angular momentum operator in  $E_3$ , and separating variables in the solution as  $\Psi(\chi, \theta, \varphi) = \psi(\chi, \kappa) Y_l^m(\theta, \varphi)$ , the following equation in the  $\chi$  variable (hyper-angular equation) emerges,

$$\begin{aligned} \left[ -\kappa \frac{\hbar^2}{2\mu} \frac{1}{\sin^2 \chi} \frac{\partial}{\partial \chi} \left( \sin^2 \chi \frac{\partial}{\partial \chi} \right) + \mathcal{V}(\chi, \kappa) - E(\kappa) \right] \psi(\chi, \kappa) &= 0, \\ \mathcal{V}(\chi, \kappa) &= \kappa \frac{\hbar^2}{2\mu} \frac{l(l+1)}{\sin^2 \chi} + c \cot \chi. \end{aligned} \quad (11)$$

Multiplying eq. (11) by  $(-\sin^2 \chi)$  and changing variable to

$$X(\chi, \kappa) = \sin \chi \psi(\chi, \kappa), \quad (12)$$

allows to cast it into the form of the following one-dimensional Schrödinger equation in the angular variable  $\chi$ ,

$$\left[ -\kappa \frac{\hbar^2}{2\mu} \frac{d^2}{d\chi^2} + \mathcal{V}(\chi, \kappa) \right] X(\chi, \kappa) = \left( E(\kappa) + \kappa \frac{\hbar^2}{2\mu} \right) X(\chi, \kappa). \quad (13)$$

This is precisely the equation first obtained by Schrödinger [23]. Before proceeding further, it is quite instructive to first take a close look on the free particle motion on  $S_R^3$ , i.e.  $c = 0$ , a subject treated in the next section.

## 3 Confinement phenomena as infinite barriers due to curvature: The scenarios

### 3.1 Confinement as centrifugal barrier of free particle motion on $S_R^3$

For a free particle motion on  $S_R^3$  equation (13) reduces to

$$\left[ -\kappa \frac{\hbar^2}{2\mu} \frac{d^2}{d\chi^2} + \kappa \frac{\hbar^2}{2\mu} \frac{l(l+1)}{\sin^2 \chi} \right] \mathcal{S}(\chi, \kappa) = E^{(c=0)}(\kappa) \mathcal{S}(\chi, \kappa), \quad (14)$$

with  $\mathcal{S}(\chi, \kappa)$  denoting the free-particle solution. The second term on the l.h.s. of this equation describes the centrifugal energy,  $U_l(\chi, \kappa)$ , of a particle of a non-zero orbital angular momentum on  $S_R^3$ , i.e.,

$$U_l(\chi, \kappa) = \kappa \frac{\hbar^2 l(l+1)}{2\mu \sin^2 \chi}. \quad (15)$$

This term provides an infinite barrier and thereby a confinement, an observation to acquire profound importance in what follows.

The energy spectrum of eq. (14) is easily found from the observation on its inherent  $O(4)$  symmetry. Indeed, the angular part,  $\hat{\square}$ , of the four-dimensional Laplacian,  $\square$ , represents the operator of the four-dimensional angular momentum, here denoted by  $\mathcal{K}^2$ ,<sup>1</sup> according to,  $\square = -\frac{1}{R^2}\hat{\square} = -\frac{1}{R^2}\mathcal{K}^2$ , whose action on the states is given by [39]

$$\mathcal{K}^2|K, l, m\rangle = K(K+2)|K, l, m\rangle. \quad (16)$$

Here, the  $O(4)$  states have been equipped by the quantum numbers,  $K$ ,  $l$ , and  $m$  defining the eigenvalues of the respective four-, three- and two-dimensional angular momentum operators upon same states. These quantum numbers correspond to the  $O(4)/O(3)/O(2)$  reduction chain and satisfy the branching rules,  $l = 0, 1, 2, \dots, K$ , and  $m = -l, \dots, +l$ .

Therefore, the corresponding energy spectrum has to be

$$E_K^{(c=0)}(\kappa) = \kappa \frac{\hbar^2}{2\mu} K(K+2). \quad (17)$$

When cast in terms of  $n = K + 1$ , the latter spectrum takes the form

$$E_n^{(c=0)}(\kappa) = \kappa \frac{\hbar^2}{2\mu} (n^2 - 1), \quad (18)$$

which coincides (up to an additive constant) with the spectrum of a particle confined within an infinitely deep spherical quantum-box well. Then  $n$  acquires meaning of principal quantum number.

The solutions of eq. (14) are text-book knowledge [39], [40] and rely in the following way upon the Gegenbauer polynomials,  $C_m^\alpha$ , the  $O(4)$  orthogonal polynomials,

$$\mathcal{S}_{Kl}(\chi, \kappa) = \sqrt{\kappa} 2^{l+1} l! \sqrt{\frac{\kappa(K+1)(K-l)!}{2\pi^2(K+l+1)!}} \sin^l \chi C_{K-l}^{l+1}(\cos \chi). \quad (19)$$

The complete solutions to eq. (14) and on the unit hypersphere are the well known hyper-spherical harmonics given by

$$|Klm\rangle = Z_{Klm}(\chi, \theta, \varphi) = \mathcal{S}_{Kl}(\chi, \kappa = 1) Y_l^m(\theta, \varphi), \quad (20)$$

where  $Y_l^m(\theta, \varphi)$  are the standard spherical harmonics in ordinary three space.

### 3.2 Confinement as $\cot \chi$ barrier

Various potentials in conventional flat  $E_3$  space appear as images to the  $\cot \chi$  potential in eq. (8). Their explicit forms are determined by the choice of coordinates on  $S_R^3$  which shape the line element,  $ds$ . The general expression of the line element in the space under consideration and in hyper-spherical coordinates,  $\Omega = \{\chi, \theta, \varphi\}$ , reads

$$ds^2 = \frac{1}{\kappa} [d\chi^2 + \sin^2 \chi (d\theta^2 + \sin^2 \theta d\varphi^2)]. \quad (21)$$

---

<sup>1</sup>The analogue on the two-dimensional sphere of a constant radius  $r = a$  is the well known relation  $\vec{\nabla}^2 = -\frac{1}{a^2}L^2$ .

Upon the variable substitution,  $\chi = f(r)$ , restricted to  $0 \leq f(r) \leq \pi$ , eq. (21) takes the form

$$\begin{aligned} ds^2 &= \frac{1}{\kappa} [(f'(r))^2 dr^2 + \sin^2 f(r) (d\theta^2 + \sin^2 \theta d\varphi^2)], \\ &\equiv D^2(r, \kappa) \frac{dr^2}{r^2} + \mathcal{R}^2(r, \kappa) (d\theta^2 + \sin^2 \theta d\varphi^2), \end{aligned} \quad (22)$$

$$D(r, \kappa) \equiv \frac{r}{\sqrt{\kappa}} f'(r), \quad \mathcal{R}(r, \kappa) \equiv \frac{\sin f(r)}{\sqrt{\kappa}}, \quad (23)$$

where  $D(r, \kappa)$ , and  $\mathcal{R}(r, \kappa)$  are usually referred to as ‘‘gauge metric tensor’’ and ‘‘scale factor’’, respectively [41].

Changing variable in eq. (13) correspondingly is standard and various choices for  $f(r)$  give rise to a variety of radial equations in ordinary flat space with effective potentials which are not even necessarily central. All these equations, no matter how different that may look, are of course equivalent, they have same spectra, and the transition probabilities between the levels are independent on the choice for  $f(r)$ . Nonetheless, some of the scenarios provided by the different choices for  $f(r)$  can be more efficient in the description of particular phenomena than others.

Precisely here lies the power of the curvature concept as the common prototype of confinement phenomena of different disguises. In the following we shall present two typical examples for  $f(r)$ .

### 3.2.1 The $D(r, \kappa) = \frac{r\sqrt{\kappa}}{1+r^2\kappa}$ gauge and a gradient dependent confinement potential with a position dependent reduced mass

A prominent choice for the transformation of the angular  $\chi$  variable to the  $r$  variable has been made in ref. [42] for the purpose of quantum dots physics. This gauge is of general interest in so far as in flat  $E_3$  space it describes a particle with position and curvature dependent mass moving within a confinement potential whose infinite barrier is generated by gradient terms. The transformation under consideration reads

$$\chi = \tan^{-1} r\sqrt{\kappa}, \quad 0 \leq r\sqrt{\kappa} < \infty, \quad (24)$$

and corresponds to a parametrization of the ‘‘upper’’ hemisphere in terms of tangential projective coordinates with respect to the ‘‘North’’ pole. The line element in this gauge becomes

$$ds^2 = \frac{1}{(1+r^2\kappa)^2} r^2 dr + \frac{1}{\kappa} \sin^2(\tan^{-1} r\sqrt{\kappa}) (d\theta^2 + \sin^2 \theta d\varphi^2). \quad (25)$$

The intriguing aspect of this gauge is that in the  $r$  variable the  $\cot \chi$  potential on  $S_R^3$  is portrayed by a gradient dependent potential with a position and curvature dependent reduced mass. Indeed, changing the  $\chi$  variable in the principal curved space Schrödinger wave equation in (13) in accordance with eq. (24) and upon the substitution <sup>2</sup>,

$$\psi(\tan^{-1} r\sqrt{\kappa}) = (1 + \kappa r^2) \Phi(r, \kappa), \quad (26)$$

amounts after some straightforward algebra to

$$\begin{aligned} -\frac{\hbar^2}{2\mu} (1 + \kappa r^2) \left[ (1 + \kappa r^2) \frac{\partial^2}{\partial r^2} + \frac{2}{r} (1 + 3\kappa r) \frac{\partial}{\partial r} + 6\kappa - \frac{l(l+1)}{r^2} \right] \Phi(r, \kappa) \\ + \alpha \cot(\tan^{-1} r\sqrt{\kappa}) \Phi(r, \kappa) = E(\kappa) \Phi(r, \kappa), \quad \alpha = \frac{e^2 Z}{\epsilon}. \end{aligned} \quad (27)$$

Now introducing the position and curvature dependent mass as

$$\mu^*(r, \kappa) = \frac{\mu}{1 + \kappa r^2}, \quad (28)$$

<sup>2</sup> This substitution ensures that the  $\Phi(r, \kappa)$ 's are normalized as wave functions in  $E_3$ .

plotted in Fig. 1, and accounting for the relation,  $\cot(\tan^{-1} r\sqrt{\kappa}) = 1/(r\sqrt{\kappa})$ , allows to cast eq. (27) into the following symmetrized form of the kinetic terms,

$$\left[ \frac{1}{2} \left( \frac{1}{\mu^*(r, \kappa)} \Delta_r + \Delta_r \frac{1}{\mu^*(r, \kappa)} \right) + v \left( r, \frac{\partial}{\partial r}, \kappa \right) \right] \Phi(r, \kappa) = E(\kappa) \Phi(r, \kappa). \quad (29)$$

The explicit expression for the gradient potential reads:

$$v \left( r, \frac{\partial}{\partial r}, \kappa \right) = \frac{\alpha}{r\sqrt{\kappa}} - \frac{\hbar^2 \kappa}{2\mu^*} \left[ \left( r \frac{\partial}{\partial r} \right)^2 + 3 \left( r \frac{\partial}{\partial r} \right) + 3 \right] - \frac{\hbar^2 \kappa^2}{\mu} r^2 \left( r \frac{\partial}{\partial r} + 1 \right),$$

$$\Delta_r = \frac{\partial^2}{\partial r^2} + \frac{2}{r} \frac{\partial}{\partial r} - \frac{l(l+1)}{r^2}. \quad (30)$$

Equation (29) describes particles with position and curvature dependent masses confined within a gradient potential, a scenario suited for the case of electrons confined in semi-conductor quantum dots.

This confinement phenomenon, that occurs due to the electron-crystal interaction, may not restrict to quantum dots alone. Also quarks with position dependent masses due to quark-sea interaction may be of interest too [43].

### 3.2.2 The $D(r, \kappa) = \pi r$ gauge and the central trigonometric Rosen-Morse potential

An especially simple and convenient parametrization of the  $\chi$  variable in terms of  $r$ , also used by Schrödinger [23] and corresponding to the  $D(r) = \pi r$  gauge is

$$\chi = \frac{r}{R} \pi \equiv \frac{r}{d}, \quad d = \frac{R}{\pi}, \quad \frac{r}{R} \in [0, 1], \quad \kappa \rightarrow \tilde{\kappa} = \frac{1}{d^2}, \quad (31)$$

in which case the line element takes the form

$$ds^2 = \frac{\pi^2}{\tilde{\kappa}} \left( d \left( r\sqrt{\tilde{\kappa}} \right)^2 + \sin^2 \left( r\sqrt{\tilde{\kappa}} \right) (d\theta^2 + \sin^2 \theta d\varphi^2) \right). \quad (32)$$

Here, the length parameter  $d$  assumes the rôle of rescaled hyper-radius. Correspondingly, in this particular gauge, the place of the genuine curvature,  $\kappa = 1/R^2$ , is taken by the rescaled one,  $\tilde{\kappa} = 1/d^2$ . Setting now  $c = -2G\sqrt{\tilde{\kappa}}$ , eq. (11) takes the form of a radial Schrödinger equation with a particular central potential of infinite depth (confinement potential) known in SUSYQM under the name of the *trigonometric Rosen-Morse potential (or, Rosen-Morse I)* [44]. This equation reads

$$\left[ -\tilde{\kappa} \frac{\hbar^2}{2\mu} \frac{d^2}{d \left( r\sqrt{\tilde{\kappa}} \right)^2} + \mathcal{V} \left( r\sqrt{\tilde{\kappa}}, \tilde{\kappa} \right) \right] X \left( r\sqrt{\tilde{\kappa}}, \tilde{\kappa} \right) = \left( E(\tilde{\kappa}) + \frac{\hbar^2}{2\mu} \tilde{\kappa} \right) X \left( r\sqrt{\tilde{\kappa}}, \tilde{\kappa} \right),$$

$$\mathcal{V} \left( r\sqrt{\tilde{\kappa}}, \tilde{\kappa} \right) = \tilde{\kappa} \frac{\hbar^2}{2\mu} \frac{l(l+1)}{\sin^2 \left( r\sqrt{\tilde{\kappa}} \right)} - 2G\sqrt{\tilde{\kappa}} \cot \left( r\sqrt{\tilde{\kappa}} \right). \quad (33)$$

Important to note, SUSYQM suppresses the curvature dependence of  $\mathcal{V}$  by absorbing it into the constants and the variable through the replacements,  $G\sqrt{\tilde{\kappa}} \rightarrow b$ , and  $\tilde{\kappa}l(l+1) \rightarrow a(a+1)$ , and refers to  $r\sqrt{\tilde{\kappa}}$  as to a dimensionless position variable,  $r \in [0, \pi]$ .

Besides Schrödinger, eq. (33) has been solved by various authors using different schemes. The solutions obtained in [45] are built on top of Jacobi polynomials of imaginary arguments and parameters that are complex conjugate to each other, while ref. [34] expands the wave functions of the interacting case in the free particle basis. The most recent construction in our previous work

[46] instead relies upon real Romanovski polynomials. In the  $\chi$  variable and according to eq. (12) (versus  $\psi(r) = r\mathcal{R}(r)$  in  $E_3$ ) our solutions take the form,

$$X_{(Kl)}(\chi, \tilde{\kappa}) = N_{(Kl)} \sin^{K+1} \chi e^{-\frac{b\chi}{\tilde{\kappa}+1}} R_{K-l}^{(\frac{2b}{\tilde{\kappa}+1}, -(K+1))}(\cot \chi), \quad b = \frac{2\mu G}{\sqrt{\tilde{\kappa}}\hbar^2},$$

$$K = 0, 1, 2, \dots, \quad l = 0, 1, \dots, K, \quad (34)$$

where  $N_{(Kl)}$  is a normalization constant. The  $R_n^{(\alpha, \beta)}(\cot \chi)$  functions are the non-classical Romanovski polynomials [47, 48] which are defined by the following Rodrigues formula,

$$R_n^{(\alpha, \beta)}(x) = e^{\alpha \cot^{-1} x} (1+x^2)^{-\beta+1} \times \frac{d^n}{dx^n} e^{-\alpha \cot^{-1} x} (1+x^2)^{\beta-1+n}, \quad (35)$$

where  $x = \cot r\sqrt{\tilde{\kappa}}$  (see ref. [49] for a recent review).

The energy spectrum of  $\mathcal{V}(r\sqrt{\tilde{\kappa}}, \tilde{\kappa})$  is given by

$$E_K(\tilde{\kappa}) = -\frac{G^2}{\frac{\hbar^2}{2\mu}} \frac{1}{(K+1)^2} + \tilde{\kappa} \frac{\hbar^2}{2\mu} ((K+1)^2 - 1), \quad l = 0, 1, 2, \dots, K. \quad (36)$$

Giving  $(K+1)$  the interpretation of a principal quantum number  $n = 0, 1, 2, \dots$  (as in the  $H$  atom), one easily recognizes that the energy in eq. (36) is defined by the Balmer term and its inverse of opposite sign, thus revealing  $O(4)$  as dynamical symmetry of the problem. Stated differently, particular levels bound within different potentials (distinct by the values of  $l$ ) carry same energies and align to levels (multiplets) characterized, similarly to the free case in eq. (16), by the four dimensional angular momentum,  $K$ . The  $K$ -levels belong to the irreducible  $O(4)$  representations of the type  $(\frac{K}{2}, \frac{K}{2})$ . When the confined particle carries spin-1/2, as is the case of electrons in quantum dots, or quarks in baryons, one has to couple the spin, i.e. the  $(\frac{1}{2}, 0) \oplus (0, \frac{1}{2})$  representation, to the previous multiplet, ending up with the (reducible)  $O(4)$  representation

$$|K, l, m, s = \frac{1}{2}\rangle = \left(\frac{K}{2}, \frac{K}{2}\right) \otimes \left[\left(\frac{1}{2}, 0\right) \oplus \left(0, \frac{1}{2}\right)\right]. \quad (37)$$

This representation contains  $K$  parity dyads and a state of maximal spin,  $J_{\max} = K + \frac{1}{2}$ , without parity companion and of either positive ( $\pi = +$ ) or, negative ( $\pi = -$ ) parity,

$$\frac{1^\pm}{2}, \dots, \left(K - \frac{1}{2}\right)^\pm, \left(K + \frac{1}{2}\right)^\pi \in |K, l, m, s = \frac{1}{2}\rangle. \quad (38)$$

As we shall see below this scenario turns to be the one adequate for the description of non-strange baryon structure.

The above examples are illustrative of the power of curved space potentials as sources for a variety of effective confinement potentials in ordinary flat  $E_3$  space.

However, much care is in demand when working with such potentials. One should be aware of the fact that physical observables do not depend on the gauge chosen and performing in the  $r$  variable has to be consistent with performing in the  $\chi$  variable. We shall come back to this point in the next section.

## 4 $S_R^3$ potentiology: The baryons

### 4.1 The nucleon spectrum in the $SO(4)$ symmetry scheme

The spectrum of the nucleon continues being enigmatic despite the long history of the respective studies (see refs. [50], [51] for recent reviews). Unprejudiced inspection of the data reported by

the Particle Data Group [52] reveals a systematic degeneracy of the excited states of the baryons of the best coverage, the nucleon ( $N$ ) and the  $\Delta(1232)$ . Our case is that

- levels and level splittings of the nucleon and  $\Delta$  spectra match the spectrum of in eq. (36),
  - the curvature induced confinement potential in eq. (33) is the exactly solvable extension of to the Cornell potential predicted by Lattice QCD.
1. The  $N$  and  $\Delta$  spectra: Afreque ll the observed nucleon resonances with masses below 2.5 GeV fall into the three  $K = 1, 3, 5$  levels in eq. (38) with only the two  $F_{17}$  and  $H_{1,11}$  states still “missing”, an observation due to refs. [53]. Moreover, the level splittings follow with an amazing accuracy eq. (36). This is in fact a result already reported in our previous work in ref. [17] where we assumed dominance of a quark-diquark configuration in nucleon structure, and fitted the nucleon spectrum in Fig. 2 to the spectrum of the trigonometric Rosen-Morse potential (c.f. eq. (33)) by the following set of parameters,

$$\mu = 1.06 \text{ fm}^{-1}, \quad G = 237.55 \text{ MeV} \cdot \text{fm}, \quad d = 2.31 \text{ fm}. \quad (39)$$

However, in ref. [17] the curvature concept has not been taken into consideration and because of that the  $d$  quantity did not have any deeper meaning but the one of some length matching parameter. This contrasts the present work, which in being entirely focused on the geometric aspect of confinement, places  $d$  on the firmer ground of a parameter encoding a space curvature.

Almost same set of parameters, up to a modification of  $d$  to  $d = 3$  fm, fits the  $\Delta(1232)$  spectrum, which exhibits exactly same degeneracy patterns, and from which only the three  $P_{31}, P_{33}$ , and  $D_{33}$  states from the  $K = 5$  level are “missing”. Remarkably, none of the reported states, with exception of the  $\Delta(1600)$  resonance, presumably a hybrid, drops from the systematics. The unnatural parity of the  $K = 3, 5$  levels requires a pseudoscalar diquark. For that one has to account for an  $1^-$  internal excitation of the diquark which, when coupled to its maximal spin  $1^+$ , can produce a pseudoscalar in one of the possibilities. The change of parity from natural to unnatural can be given the interpretation of a chiral phase transition in baryon spectra. Levels with  $K = 2, 4$  have been attributed to entirely “missing” resonances in both the  $N$  and  $\Delta$  spectra. To them, natural parities have been assigned on the basis of a detailed analysis of the  $1p - 1h$  Hilbert space of three quarks and its decomposition in the  $|K, l, m, s = \frac{1}{2}\rangle$  basis [53]. The  $\Delta(1232)$  spectrum obtained in this way is shown in Fig. 3. We predict a total of 33 unobserved resonances of a dominant quark-diquark configurations in the  $N$  and  $\Delta(1232)$  spectra with masses below  $\sim 2500$  MeV, much less but any other of the traditional models.

In ref. [17] mentioned above, the potential in eq. (33) has been considered in the spirit of SUSYQM as a *central two-parameter* potential in  $E_3$  and without reference to  $S_R^3$ , a reason for which the values of the parameter accompanying the  $\text{csc}^2$  term had to be taken as integer *ad hoc* and for the only sake of a better fit to the spectra, i.e., without any deeper justification. Instead, in the present work,

we fully recognize that the higher dimensional potential  $\mathcal{V}(\chi, \kappa)$  in eq. (13), which acts as the prototype of Rosen-Morse I, is a *non-central one-parameter* potential in which the strength of the  $\text{csc}^2$  term, the centrifugal barrier on  $S_R^3$ , is uniquely fixed by the eigenvalues of underlying three-dimensional angular momentum.

2. Relationship to QCD dynamics: The convenience of the scenario under consideration is additionally backed by the fact that the Cornell quark confinement potential [13] predicted by Lattice QCD [12] is no more but the small-angle approximation to  $\cot r\sqrt{\tilde{\kappa}}$  in eq. (8). Indeed, the first terms of the series expansion are

$$-2G\sqrt{\tilde{\kappa}} \cot r\sqrt{\tilde{\kappa}} + \tilde{\kappa} \frac{\hbar^2}{2\mu} \frac{l(l+1)}{\sin^2(r\sqrt{\tilde{\kappa}})} \approx -\frac{2G}{r} + \frac{2G\tilde{\kappa}}{3}r + \frac{\hbar^2}{2\mu} \frac{l(l+1)}{r^2}, \quad (40)$$

with  $\tilde{\kappa} = \frac{1}{a^2} = \frac{\pi^2}{R^2}$ .

Therefore,  $\mathcal{V}(r\sqrt{\tilde{\kappa}}, \tilde{\kappa})$ , is the exactly solvable *trigonometric extension to the Cornell* potential, a reason for which we shall frequently refer to  $\mathcal{V}(r\sqrt{\tilde{\kappa}}, \tilde{\kappa})$  as TEC potential.

Finally, the ‘‘curved’’  $1/r$  potential has been completely independently used in [41] within the context of charmonium physics. However, in refs. [41] at the end the degeneracy of the states has been removed through an *ad hoc* extension of the Hamiltonian to include an additional  $L^2/r^2$ -term of sign opposite to four-dimensional centrifugal barrier,  $L^2/\sin^2\chi$ , so that all states with  $l = 1, 2, \dots, K$  could be pushed below the  $S$  state belonging to a given  $K$ . In this way a better description of the charmonium states has been achieved indeed but on the cost of compromising consistency of the geometric  $S_R^3$  concept. In contrast to the charmonium, in  $N$  and  $\Delta(1232)$  baryon spectra the  $S_R^3$  degeneracy patterns are pretty well pronounced especially in the most reliable region below 2000 MeV where our predicted  $K = 1, 3$  levels in the  $\Delta$  spectrum appear even complete. This occasion allows to maintain the  $S_R^3$  geometric concept intact and the exact wave functions unaltered, so far. In subsection C below these wave functions will be put at work in the description of the mean square proton charge radius.

## 4.2 The nucleon spectrum in the $SO(2, 1)$ symmetry scheme

The energy spectrum in eq. (36) can equivalently be cast in terms of the eigenvalues of the  $SO(2, 1)$  Casimir, the pseudo-angular momentum operator,  $\mathcal{J}^2 = -J_\pm J_\mp + J_0^2 \pm J_0$  [19],[20]. Here, the operators  $J_\pm$  and  $J_0$  satisfy the group algebra  $[J_+, J_-] = -2J_0$ , and  $[J_0, J_\pm] = \pm J_\pm$ . The eigenstates are labeled by the quantum numbers  $j$ , and  $m'$  which define the respective eigenvalues of  $\mathcal{J}^2$  and  $J_0$  according to  $J_0|j, m'\rangle = m'|j, m'\rangle$ , and  $\mathcal{J}^2|j, m'\rangle = \left((j - \frac{1}{2})^2 - \frac{1}{4}\right)|j, m'\rangle$ , respectively.

The group  $SO(2, 1)$ , in being non-compact, allows only for infinite dimensional unitary representations labeled as  $D_j^{\pm(m')}$  where the positive, and negative upper signs refer in their turn to  $m'$  values limited from either below,  $m' = j + n$  with  $n$  non-negative integer, or above,  $m' = j - n$  where we used a nomenclature of positive integer or half-integer  $j$  (also known as Bargmann index).

Back to eq. (36), it is not obvious how to re-express the general two-term energy formula containing both the quadratic and inverse quadratic eigenvalues of the  $SO(4)$  Casimir in terms of  $SO(2, 1)$  quantum numbers. The most obvious option consists in nullifying the potential strength, i.e. setting  $G = 0$ , which takes one back to the free particle on the hypersphere. In this case only the quadratic terms survives which is easily equivalently rewritten to

$$E_j(\tilde{\kappa}) = \tilde{\kappa} \frac{\hbar^2}{2\mu} \left( (m')^2 - 1 \right), \quad j = l + 1, \quad m' = j + n, \quad (41)$$

where  $l$  is the ordinary angular momentum label, while  $n$  is the radial quantum number (it equals the order of the polynomial shaping the wave function labeled by  $K$  in eq. (34)). The  $m'$  label is limited from below and the whole spectrum can be associated with the basis of the infinite unitary  $SO(2, 1)$  representation,  $D_j^+(m')$ . It is obvious that the degeneracy patterns in the  $SO(2, 1)$  spectrum designed in this manner are same as the  $SO(4)$  ones.

Perhaps nothing expresses the  $SO(2, 1)/SO(4)$  symmetry correspondence better but this extreme case in which the manifestly  $SO(4)$  symmetric centrifugal energy on the ( $3D$ ) hypersphere is cast in terms of  $SO(2, 1)$  pseudo-angular momentum values.

Although the bare  $l(l+1)$  csc<sup>2</sup> potential is algebraically in line with  $AdS_5/CFT$  correspondence, it completely misses the perturbative aspect of QCD dynamics. The better option for getting rid of the inverse-quadratic term in eq. (36) is to permit  $K$  dependence of the potential strength and choose  $G = g(K + 1)$  with  $g$  being a new free parameter. Such a choice (up to notational differences) has been made in [21]. If so, then the energy takes the form

$$E_j(\tilde{\kappa}) = -g^2 \frac{\hbar^2}{2\mu} + \tilde{\kappa} \frac{\hbar^2}{2\mu} \left( (m')^2 - 1 \right), \quad j = 1, 2, 3, \dots \quad (42)$$

The above manipulation does not affect the degeneracy patterns as it only provokes a shift in the spectrum by a constant. Compared to eq. (41) the new choice allows the former inverse quadratic term to still keep presence as a contribution to the energy depending on a free constant parameter,  $g$ . In this manner, the  $SO(2, 1)$  energy spectrum continues being described by a two-term formula, a circumstance that allows for a best fit to the  $SO(4)$  description.

Once having ensured that the  $SO(2, 1)$  and  $SO(4)$  spectra share same degeneracy patterns, one is only left with the task to check consistency of the level splittings predicted by the two schemes. Comparison of eqs. (36) and (42) shows that for the high-lying levels where the inverse quadratic term becomes negligible, both formulas can be made to coincide to high accuracy by a proper choice for  $g$ . That very  $g$  parameter can be used once again to fit the low lying levels to the  $SO(4)$  description, now by a value possibly different from the previous one.

This strategy allows to make the  $SO(2, 1)$  and  $SO(4)$  descriptions of non-strange baryon spectra sufficiently close and establish the symmetry correspondence. In that manner we confirm our statement quoted in the introduction that the TEC potential is in line with both the algebraic aspects of  $AdS_5/CFT$  and QCD dynamics and provides a bridge between them.

### 4.3 The proton mean square charge radius

In this section we shall test the potential parameters in eq. (39) and the wave function in eqs. (12), (34) in the calculation of the proton electric form-factor, the touch stone of any spectroscopic model. As everywhere through the paper, the internal nucleon structure is approximated by a quark-diquark configuration. In conventional three-dimensional flat space the electric form factor is defined in the standard way [54] as the matrix element of the charge component,  $J_0(\mathbf{r})$ , of the proton electric current between the states of the incoming,  $\mathbf{p}_i$ , and outgoing,  $\mathbf{p}_f$ , electrons in the dispersion process,

$$G_E^p(|\mathbf{q}|) = \langle \mathbf{p}_f | J_0(\mathbf{r}) | \mathbf{p}_i \rangle, \quad \mathbf{q} = \mathbf{p}_i - \mathbf{p}_f. \quad (43)$$

The mean square charge radius is then defined in terms of the slope of the electric charge form factor at origin and reads,

$$\langle \mathbf{r}^2 \rangle = -6 \frac{\partial G_E^p(|\mathbf{q}|)}{\partial |\mathbf{q}|^2} \Big|_{|\mathbf{q}|^2=0}. \quad (44)$$

On  $S_R^3$ , the three-dimensional radius vector,  $\mathbf{r}$ , has to be replaced by,  $\bar{\mathbf{r}}$  with  $|\bar{\mathbf{r}}| = R \sin \chi = \sin \chi / \sqrt{\kappa}$  in accordance with eqs. (7). The evaluation of eq. (43) as four-dimensional Fourier transform requires the four-dimensional plane wave,

$$e^{iq \cdot \bar{x}} = e^{i|\mathbf{q}||\bar{\mathbf{r}}| \cos \theta} = e^{i|\mathbf{q}| \frac{\sin \chi}{\sqrt{\kappa}} \cos \theta}, \quad |\bar{\mathbf{r}}| = R \sin \chi = \frac{\sin \chi}{\sqrt{\kappa}}. \quad (45)$$

The latter refers to a  $z$  axis chosen along the momentum vector (a choice justified in elastic scattering<sup>3</sup>), and a position vector of the confined quark having in general a non-zero projection on the extra dimension axis in  $E_4$ .

The integration volume on  $S_R^3$  is given by  $\sin^2 \chi \sin \theta d\chi d\theta d\varphi$ . The explicit form of the nucleon ground state wave function obtained from eq. (34) in the  $\chi$  variable reads

$$\begin{aligned} X_{(00)}(\chi, \tilde{\kappa}) &= N_{(00)} e^{-b\chi} \sin \chi, \\ N_{(00)} &= \frac{4b(b^2 + 1)}{1 - e^{-2\pi b}}, \quad b = \frac{2\mu G}{\sqrt{\tilde{\kappa}} \hbar^2}. \end{aligned} \quad (46)$$

With that, the charge-density takes the form,  $J_0(\chi, \tilde{\kappa}) = e_p |\psi_{\text{gst}}(\chi, \tilde{\kappa})|^2$ ,  $e_p = 1$ . In effect, eq. (43) amounts to the calculation of the following integral,

$$G_E^p(|\mathbf{q}|, \tilde{\kappa}) = \sqrt{\kappa} \int_0^\pi d\chi \frac{(X_{(00)}(\chi, \tilde{\kappa}))^2 \sin(|\mathbf{q}| \frac{\sin \chi}{\sqrt{\kappa}})}{|\mathbf{q}| \sin \chi}, \quad (47)$$

<sup>3</sup>A consistent definition of the four-dimensional plane wave in  $E_4$  would require an Euclidean  $q$  vector. However, for elastic scattering processes, of zero energy transfer, where  $q_0 = 0$ , the  $q$  vector can be chosen to lie entirely in  $E_3$ , and be identified with the physical space-like momentum transfer.

Table 1: Best fit values for the  $S_R^3$  curvature.

	hyper-radius $R$	$\kappa = \frac{1}{R^2}$	rescaled hyper-radius $d = \frac{R}{\pi}$	$\tilde{\kappa} = \frac{1}{d^2}$
$N$ spectrum	7.26 fm	0.019 fm <sup>-2</sup>	2.31 fm	0.187 fm <sup>-2</sup>
$\Delta$ spectrum	9.42 fm	0.011 fm <sup>-2</sup>	3 fm	0.11 fm <sup>-2</sup>
form factor	10.46 fm	0.009 fm <sup>-2</sup>	3.33 fm	0.090 fm <sup>-2</sup>

where the dependence of the form factor on the curvature has been indicated explicitly.

The integral is taken numerically and the resulting charge form factor of the proton is displayed in Fig. 4 together with data. The best fit values for  $R$  (equivalently,  $d$ ), and the related curvatures are given in Table 1, for illustrative purpose. The best fit value of the mean square charge radius is found as

$$\langle \mathbf{r}^2 \rangle = 0.87 \text{ fm}^2, \quad (48)$$

and reproduces well the corresponding experimental value of  $\langle \mathbf{r}^2 \rangle_{\text{exp}} = 0.8750 \text{ fm}^2$  [52]. We further observe that our best fit is of the quality of the calculation of same observable within the framework of the Bethe-Salpeter equation based upon an instanton induced two-body potential [55].

A comment is in order on how the present result compares to our previous work [17] where same observable has been calculated without reference to the curvature concept. There, the corresponding Schrödinger equation (with essentially same potential) has been written in terms of the three-dimensional Laplacian versus four-dimensional in the present work. Using eq. (33) it can be shown that the  $E_3$  form factor in ref. [17] represents the small  $\chi$  limit,  $\sin \chi \approx \chi$  with  $\chi = r\sqrt{\tilde{\kappa}}$ , of the  $S_R^3$  case, an occasion that allowed to take it in closed form. Comparing the  $E_3$  to the  $S_R^3$  calculation reveals the insignificant differences shown in Figs. 5, and 5. The coincidence is due to the rapid exponential fall of the ground state wave function in eq. (46) which strongly damps the large  $\chi$  angle contributions to the integral in eq. (47) (c.f. Fig. 6).

The result shows that specifically in the  $D(r, \kappa) = \pi r$  gauge,

- performing in  $E_3$  is consistent with performing on  $S_R^3$  in the small  $\chi$  angle limit, in which  $\sin \chi \approx \chi$  with  $\chi = r\sqrt{\tilde{\kappa}}$ ,
- the proton charge electric form-factor is not sufficiently a sensitive observable toward the curvature parameter.

This contrasts excited states whose wave functions for  $l > 0$  show non-negligible large  $\chi$  angle dependences (c.f. Fig. 6) in which case the Fourier transforms on  $S_R^3$  will become distinguishable from those in  $E_3$ . This is visualized in Fig. 7 by the electric charge form-factor for an  $l = 2$  state from the second observed level with  $K = 3$  which corresponds to the first  $F_{15}$  resonance.

## 5 Curvature shut-down: The deconfinement

The presence of the curvature parameter in the trigonometrically extended Cornell confinement potential opens an intriguing venue toward deconfinement as a  $S_R^3$  curvature shut-down. It can be shown that

high-lying bound states from the trigonometrically extended Cornell confinement potential approach scattering states of the Coulomb-like potential in ordinary flat space. Stated differently, the TEC confinement gradually fades away with vanishing curvature and allows for deconfinement.

The latter is most easily demonstrated for the case of a TEC potential with a nullified  $G$  parameter and reduced to the  $\text{csc}^2$  term, the  $S_R^3$  centrifugal barrier. Indeed, for small curvatures such that  $K\sqrt{\kappa} \sim k$ , with “ $k$ ” a constant, eq. (18) goes into

$$E_K^{(c=0)}(\kappa) \xrightarrow{\kappa \rightarrow 0} \frac{\hbar^2}{2\mu} k^2, \quad (49)$$

and describes a continuous energy spectrum. Moreover, in parallel with the asymptotic behavior of the energy spectrum in eq. (49), also the wave functions from the confinement phase,  $\mathcal{S}_{Kl}(\chi, \kappa)$ , approach in same limit the wave functions relevant for the deconfinement phase which are the scattering states of the inverse distance potential in flat  $E_3$  space. In order to see this it is useful to recall the following differential recursive relation satisfied by the  $\mathcal{S}_{Kl}$  functions [34],

$$\begin{aligned} \mathcal{S}_{Kl}(\chi, \kappa) &= \frac{\sin^l \chi}{\sqrt{(n^2 - 1) \dots (n^2 - l^2)}} \frac{d^l}{(d \cos \chi)^l} \mathcal{S}_{K0}(\chi, \kappa), \\ \mathcal{S}_{K0}(\chi, \kappa) &= \sqrt{\frac{2\kappa}{\pi}} \frac{\sin(K+1)\chi}{\sin \chi}. \end{aligned} \quad (50)$$

In the limits when  $\kappa \rightarrow 0$ , and  $\chi \rightarrow 0$  in such a way that  $\chi/\sqrt{\kappa}$  stays finite and approaches  $\chi/\sqrt{\kappa} \rightarrow r$  (here, the factor  $\pi$  has been absorbed by  $r$  for simplicity), while  $K\sqrt{\kappa} \rightarrow k$  with a constant “ $k$ ”, i.e.,

$$\lim_{\kappa \rightarrow 0} (K+1)\sqrt{\kappa} \rightarrow k, \quad \lim_{\kappa \rightarrow 0} \frac{\chi}{\sqrt{\kappa}} \rightarrow r, \quad (51)$$

one also finds

$$\begin{aligned} \sin(K+1)\chi &\rightarrow \sin(K+1)\sqrt{\kappa}r \rightarrow \sin kr, & \sin \chi &\rightarrow \sqrt{\kappa}r, \\ d \cos \chi &= -\sin \chi d\chi \rightarrow -\kappa r dr. \end{aligned} \quad (52)$$

Accounting for the latter relations, eq. (50) takes the form of the Reyleigh formula [35] for the spherical Bessel functions,

$$\begin{aligned} \lim_{\kappa \rightarrow 0} \mathcal{S}_{Kl}(\chi, \kappa) &\rightarrow \sqrt{\frac{2k^2}{\pi}} (-1)^l (kr)^l \left( \frac{1}{kr} \frac{d}{d(kr)} \right)^l \frac{\sin kr}{kr} \\ &= \sqrt{\frac{2k^2}{\pi}} j_l(kr). \end{aligned} \quad (53)$$

The latter wave functions are precisely the ones that describe scattering states in ordinary flat  $E_3$  space, i.e., they are the radial functions in the Helmholtz equation describing free motion in  $E_3$ . This example, though a very simplistic one, is already illustrative of the effect that the curvature shut-down can have as deconfinement mechanism.

In the presence of the  $\cot \chi$  barrier the spectrum is shaped after eq. (36). In the unconditional  $\kappa \rightarrow 0$  limit, the second term of the r.h.s. vanishes and the spectrum becomes the one of  $H$  atom-like bound states. In the conditional  $\sqrt{\kappa}K \rightarrow k$  limit from above, where “ $k$ ” is a constant, the term in question approaches the scattering continuum. In effect, the  $\mathcal{V}(\chi, \kappa)$  spectrum collapses down to the regular Coulomb-like potential,

$$E_K(\kappa) \xrightarrow{\kappa \rightarrow 0} -\frac{G^2}{2\mu} \frac{1}{n^2} + \frac{\hbar^2}{2\mu} k^2, \quad l = 0, 1, 2, \dots, n-1. \quad (54)$$

The rigorous proof that also the wave functions the complete TEC potential collapse to those of the corresponding Coulomb-like problem for vanishing curvature is a bit more involved and can be found in [26], [34].

In other words, as curvature goes down as it can happen because of its thermal dependence, confinement fades away, an observation that is suggestive of a deconfinement scenario controlled by the curvature parameter of the TEC potential.

Deconfinement as gradual flattening of space has earlier been considered by Takagi [7]. Compared to [7], our scheme brings the advantage that the flattening of space is paralleled by a temperature evolution of the curved TEC– to a flat Coulomb-like potential, and correspondingly, by the temperature evolution of the TEC wave functions from the confined to the Coulomb-like wave-functions from the deconfined phases, in accordance with eqs. (53), and (54).

## 6 Summary

We emphasized importance of designing confinement phenomena in terms of infinite potential barriers emerging on curved spaces. Especially, quark confinement and QCD dynamics have been modeled in terms of a trigonometric potential that emerges as harmonic potential on the three-dimensional hypersphere of constant curvature, i.e., a potential that satisfies the Laplace-Beltrami equation there. The potential under consideration interpolates between the  $1/r$ - and infinite well potentials while passing through a region of linear growth. This trigonometric confinement potential is exactly solvable at the level of the Schrödinger equation and moreover, contains the Cornell potential predicted by Lattice QCD and topological field theory [56],[57], [58] as leading terms of its Taylor decomposition. When employed as a quark-diquark potential, it led to a remarkably adequate description of the  $N$  and  $\Delta$  spectra in explaining their  $O(4)/SO(2,1)$  degeneracy patterns, level splittings, number of states, and proton electric charge-form factor. Moreover, the trigonometrically extended Cornell (TEC) potential, in carrying simultaneously the  $SO(4)$  and  $SO(2,1)$  symmetries (as the  $H$  atom!), matches the algebraic aspects of  $AdS_5/CFT$  correspondence and establishes its link to QCD potentiology. A further advantage of the TEC potential is the possibility to employ its curvature parameter, considered as temperature dependent, as a driver of the confinement-deconfinement transition in which case the wave functions of the confined phase approach bound and scattering states of ordinary flat space  $1/r$  potential.

All in all, we view the concept of curved spaces as a promising one especially within the context of quark-gluon dynamics.

### Acknowledgments

One of us (M.K) acknowledges hospitality by the Argonne National Laboratory in April 2008 and stimulating interest and discussions with T.S.H. Lee. We thank M. Krivoruchenko for providing access to ref. [41] and Nora Breton for assistance in clarifying some aspects of  $AdS_5$  gravity. Work supported by CONACyT-México under grant number CB-2006-01/61286.

## References

- [1] A. Gersten, *Euclidean special relativity*, Found. Phys. **33**, 1237-1252 (2003).
- [2] J. F. Cariñena, M. F. Rañada, M. Santander, *Superintegrability on curved spaces, orbits and momentum hodographs: revisiting a classical result by Hamilton*, J. Phys. A:Math.Theor. **40**, 13645-13666 (2007).
- [3] J. M. Nester, *Gravity, Torsion, and Gauge Theories*, in “Chalk River 1983”, Proceedings “An Introduction to Kaluza-Klein Theories”, pp. 83-115 (1983).
- [4] T. G. Vosmishcheva, A. A. Oshemkov, *Topological analysis of the two-center problem on the two-dimensional sphere*, Sbornik:Mathematics **193**, 1103-1138 (2002).
- [5] Abdus Salam, J. Strathdee, *Confinement through tensor gauge fields*, Phys. Rev. **18**, 4596-4609 (1978).
- [6] C. Dullemond, T. A. Rijken, E. van Beveren, *Quark-gluon model with conformal symmetry*, Il Nuovo Cimento A **80**, 401-428 (1984);  
I. Bediaga, M. Gaseprini, E. Predazzi, *Thermal expansion and critical temperature in a geometric representation of quark deconfinement*, Phys. Rev. D **38**, 1626-1627 (1988);  
M. Gürses, *New class of  $f - g$  fields relevant to quark confinement*, Phys. Rev. D **20**, 1019-1021 (1979);  
Saulo Carneiro, *The large numbers hypothesis and quantum mechanics*, Found.Phys.Lett. **11**, 95-103 (1998).
- [7] F. Takagi, *Quark deconfinement at finite temperature in the bag model*, Phys. Rev. D **35**, 2226-2229 (1987).
- [8] J. Maldacena, *The large  $N$  limit of superconformal field theory and supergravity*, Adv. Theor. Math. Phys. **2**, 231-252 (1998); Int. J. Theor. Phys. **38** 1113-1133 (1999).
- [9] Guy F. de Téramond, S. J. Brodsky, *Hadronic spectrum of holographic dual of QCD*, Phys. Rev. Lett. **94**, 201601-1-4 (2005).
- [10] G. S. Bali, QCD Potentiology, *\*Wien 2000, Quark confinement and the hadron spectrum\**, 209-220 (2000); e-Print: hep-ph/0010032
- [11] N. Brambilla, A. Vairo, Th. Rosch, *Effective field theory Lagrangians for baryons with two and three heavy quarks*, Phys.Rev.D **72**, 034021 (2005);  
N. Brambilla, *Effective Field Theories for  $Q Q Q$  and  $Q Q q$  baryons*, AIP Conf.Proc.**756**,366-368 (2005).
- [12] T. T. Takahashi, H. Suganuma, Y. Nemoto, H. Matsufuru, *Detailed analysis of the three-quark potential in  $SU(3)$  lattice QCD*, Phys. Rev. D **65**, 114509-1-19 (2002).
- [13] E. Eichten, H. Gottfried, T. Kinoshita, K. D. Lane, T.M. Yan, *Charmonium:The model*, Phys. Rev. D **17**, 3090-3117 (1978);  
E. Eichten, H. Gottfried, T. Kinoshita, K. D. Lane, T.M. Yan, *Charmonium:Comparison with experiment*, Phys. Rev. D **21**, 203-233 (1980).
- [14] Quarkonium Working Group (N. Brambilla et al.), *Heavy quarkonium physics*, CERN Yellow Report, CERN-2005-005, Geneva: CERN, (2005); e-Print: hep-ph/0412158
- [15] P. Gonzalez, J. Vijande, A. Valcarce, H. Garcilazo, *Spectral patterns in the nonstrange baryon spectrum*, Eur.Phys.J. A **29**, 235-244 (2006).
- [16] H. Garcilazo, *Momentum-space Faddeev calculations for confining potentials*, Phys. Rev. C **67**, 055203-1-9 (2003).

- [17] C. B. Compean, M. Kirchbach, *Trigonometric quark confinement potential of QCD traits*, Eur. Phys. J. A **33**, 1-4 (2007).
- [18] J. Fischer, J. Niederle, R. Raczka, *Generalized Spherical Functions for the Noncompact Rotation Groups*, J. Math. Phys. **7**, 816-821 (1966)
- [19] Brian G. Wybourne, *Classical groups for physicists* (Wiley-Inter-science, N.Y., 1974).
- [20] M. Novaes, *Some basics of  $su(1, 1)$* , Revista Brasileira de Ensino de Fisica **26**, 351-357 (2004).
- [21] R. Koc, M. Koca, *A systematic study on the exact solution of the position dependent mass Schrödinger equation*, J. Phys. A:Math.Gen. **36**, 8105-8112 (2003).
- [22] M. Bañados, A. Gomberoff, C. Martinez, *Anti-de Sitter space and black holes*, Class. Quantum Gravity **15**, 3575-3598 (1998).
- [23] E. Schrödinger, *A method of determining quantum mechanical eigenvalues and eigenfunction*, Proc. Roy. Irish Acad. A **46**, 9-16 (1940).
- [24] P. W. Higgs, *Dynamical symmetries in spherical geometry*, J. Phys. A:Math.Gen. **12**, 309-323 (1979).
- [25] H. I. Leemon, *Dynamical symmetries in a spherical geometry II*, J. Phys. A:Math.Gen. **12**, 489-501 (1979).
- [26] A. O. Barut, Taj Wilson, *On the dynamical group of the Kepler problem in a curved space of constant curvature*, Phys. Lett. A **110**, 351-354 (1985);  
A. O. Barut, A. Inomata, G. Junker, *Path integral treatment of the hydrogen atom in a curved space of constant curvature*, J. Phys. A:Math.Gen. **20**, 6271-6280 (1987).
- [27] L. Infeld, *On a new treatment of some eigenvalue problems*, Phys. Rev. **59**, 737-747 (1941);  
L. Infeld, A. Schild, *A note on the Kepler problem in a space of constant negative curvature*, Phys. Rev. **67**, 121-122 (1945);  
L. Infeld, T. E. Hull, *The factorization method*, Rev. Mod. Phys. **23**, 21-68 (1951).
- [28] E. Witten, *Dynamical breaking of supersymmetry*, Nucl. Phys. B **188**, 513-590 (1981).
- [29] N. Bessis, G. Bessis, *Electronic wave functions in a space of constant curvature*, J. Phys. A:Math.Gen. **12**(11), 1991-1997 (1979);  
N. Bessis, G. Bessis, D. Roux, *Space-curvature effects in the interaction between atoms and external fields: Zeeman and Stark effects in a space of constant positive curvature*, Phys. Rev. A **33**, 324-336 (1986).
- [30] Yu. Kurochkin, Dz. Shoukavy, *The tunnel-effect in the Lobachevsky space*, Acta Physica Polonica B **37**, 2423-2431 (2006);  
V. V. Gritsev, Ya. A. Kurochkin, V. S. Otchik, *Nonlinear symmetry algebra of the MIC-Kepler problem on the sphere  $S^3$* , J. Phys. A:Math.Gen. A **33**, 4903-4910 (2000).
- [31] J. Boer, F. Harmsze, T. Tijn, *Non-linear finite W symmetries and applications in elementary systems*, Phys. Rep. **272**, 139- 214 (1996).
- [32] A. Ballesteros, F. J. Herranz, *The Kepler problem on 3D spaces of variable and constant curvature from quantum algebras*, "Workshop in honor of Prof. José F. Cariñena, "Groups, Geometry and Physics", December 9-10, 2005, Zaragoza (Spain); math-ph/0604009 (2006).
- [33] Pinaki Roy, Rajkumar Roychoudhury, *Supersymmetry in curved space*, Phys. Rev. D **34**, 1787-1790 (1986).

- [34] S. I. Vinitzky, L. G. Mardoian, G. S. Pogosyan, A. N. Sissakian, T. A. Strizh, *A hydrogen atom in curved space. Expansion over free solutions on the three dimensional sphere*, Phys. Atom. Nucl. **56**, 321-327 (1993);  
V. N. Pervushin, G. S. Pogosyan, A. N. Sissakian, S. I. Vinitzky, *Equation for quasi-radial functions in momentum representation on a three-dimensional sphere*, Phys. Atom. Nucl. **56**, 1027-1043 (1993).
- [35] G. B. Arfken, H.-J. Weber, *Mathematical Methods for Physicists*, Fifth-Edition (Academic Press, N.Y., 2001).
- [36] D. Bonatsos, C. Daskaloyannis, K. Kokkotas, *Deformed oscillator algebras for two-dimensional quantum super-integrable systems*, Phys. Rev. A **50**, 3700-3709 (1994).
- [37] A. Del Sol Mesa, C. Quesne, *Connection between type A and E factorizations and construction of satellite algebras*, J. Phys. A:Math.Gen. **33**, 4059-4071 (2000).
- [38] C. C. Barros Jr., *Space-time and hadrons*, Braz. J. Phys. **37**, 17-19 (2007).
- [39] Y. S. Kim, M. E. Noz, *Theory and application of the Poincaré group* (D. Reidel, Dordrecht, 1986).
- [40] Taco Nieuwenhuis, J. A. Tjon,  *$O(4)$  Expansion of the ladder Bethe-Salpeter equation*, Few Body Syst. **21**, 167-185 (1996).
- [41] A. A. Ismest'ev, *Exactly solvable potential model for quarkonia*, Sov. J. Nucl. Phys. **52**, 1066-1076 (1990).
- [42] V. V. Gritsev, Yu. A. Kurochkin, *Model of excitations in quantum dots based on quantum mechanics in spaces of constant curvature*, Phys. Rev. B **64**, 035308-1-9 (2001).
- [43] Ravit Efraty, *Self-intersection, axial anomaly and the string picture of QCD*, Phys. Lett. B **322**, 184-190 (1994).
- [44] R. De, R. Dutt, U. Sukhatme, *Mapping of shape invariant potentials under point canonical transformations*, J. Phys. A:Math.Gen. **25**, L843-L850 (1992).
- [45] A. F. Stevenson, *Note on the "Kepler Problem" in a spherical space, and the factorization method of solving eigenvalue problems*, Phys. Rev. **59**, 842-843 (1941).
- [46] C. B. Compean, M. Kirchbach, *The trigonometric Rosen-Morse potential in the supersymmetric quantum mechanics and its exact solutions*, J. Phys. A:Math.Gen. **39**, 547-557 (2006).
- [47] E. J. Routh, *On some properties of certain solutions of a differential equation of second order*, Proc. London Math. Soc. **16**, 245 (1884).
- [48] V. Romanovski, *Sur quelques classes nouvelles de polynomes orthogonaux*, C. R. Acad. Sci. Paris, **188**, 1023-1025 (1929).
- [49] A. Raposo, H. J. Weber, D. E. Alvarez-Castillo, M. Kirchbach, *Romanovski polynomials in selected physics problems*, C. Eur. J. Phys. **5**, 253-284 (2007).
- [50] V. D. Burkert, T. S. H. Lee, *Electromagnetic meson production in the nucleon resonance region*, Int. J. Mod. Phys. E **13**, 1035-1112 (2004).
- [51] S. S. Afonin, *Parity doublets in particle physics*, Int. J. Mod. Phys. A **22**, 4537-4586 (2007).
- [52] S. Eidelman et al., *Review of particle physics*, Phys. Lett. B **592**, 1-1109 (2004).

- [53] M. Kirchbach, *On the parity degeneracy of baryons*, Mod. Phys. Lett. A **12**, 2373-2386 (1997);  
M. Kirchbach, *Classifying reported and “missing” resonances according to their P and C properties*, Int. J. Mod. Phys. A **15**, 1435-1451 (2000);  
M. Kirchbach, M. Moshinsky, Yu. F. Smirnov, *Baryons in  $O(4)$  and vibron model*, Phys. Rev. D **64**, 114005-1–11 (2001).
- [54] J. Arrington, C. D. Roberts, J. M. Zanotti, *Nucleon electromagnetic form factors*, J. Phys. G:Nucl.Part. **34**, S23-S52 (2007).
- [55] B. Metsch, <http://www.itkp.uni-bonn.de/~metsch/jlab2004>
- [56] G. t’Hooft, *On the phase transition towards permanent quark confinement*, Nucl. Phys. B **138**, 1-25 (1979).
- [57] E. Witten, *Quantum field theory and the Jones polynomial*, Comm. Math. Phys. **121**, 351 (1989); IASSNS-HEP-88/33.
- [58] H. Reinhardt, C. Feuchter, *Yang-Mills wave functional in Coulomb gauge*, Phys. Rev. D **71**, 105002-1–6 (2005).
- [59] K. Holland, P. Minkowski, M. Pape, U.-J. Wiese, *Exceptional confinement in  $G(2)$  theory*, Nucl. Phys. B **668**, 207-236 (2003).

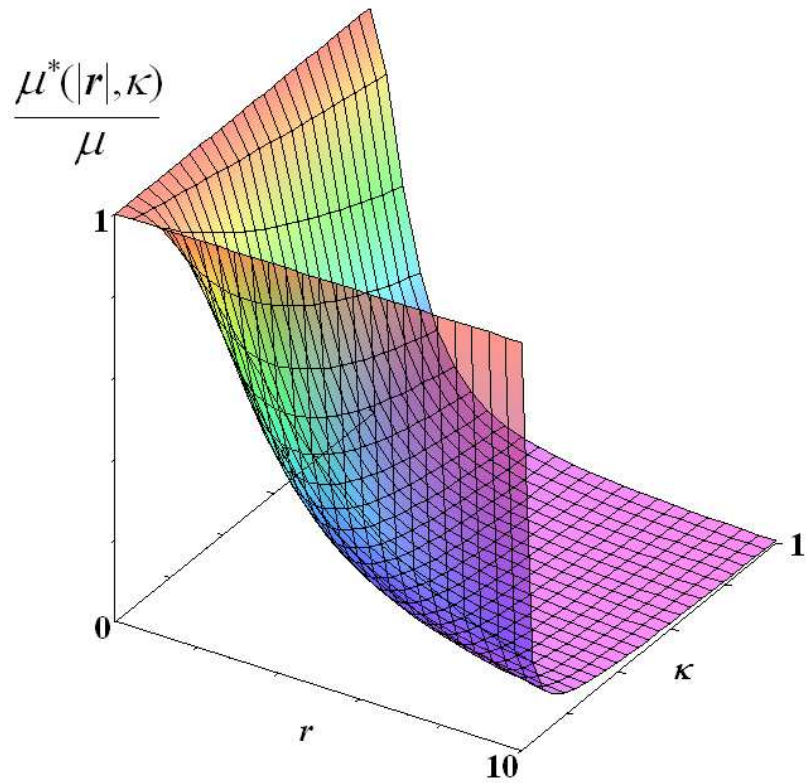


Figure 1: Position and curvature dependence of the reduced mass  $\mu^*(r, \kappa)$ . Besides effective electron masses in quantum dots, one may entertain applicability of this scenario to evolution of finite valence to vanishing parton quark masses as effect of transversal (relative to the extra dimension) displacement on the three-dimensional “plane” tangential to the “North” pole of the hemisphere.

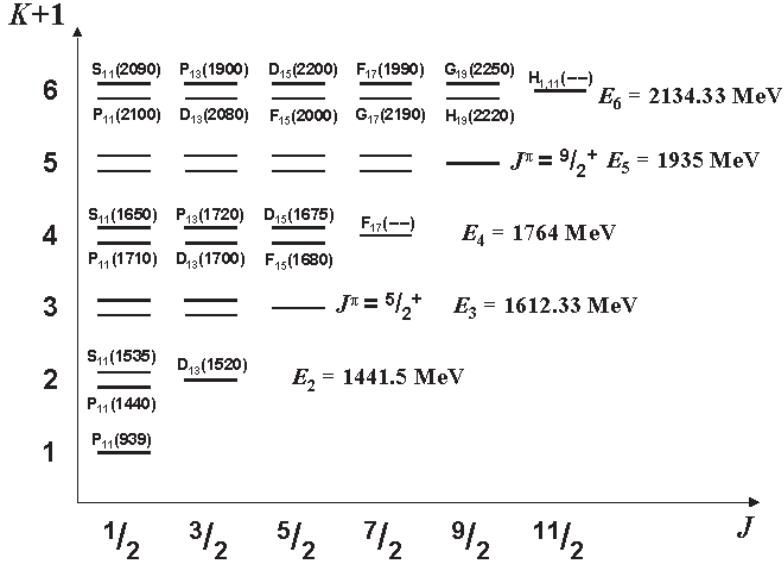


Figure 2: Assignments of the reported  $N$  excitations to the  $K$  levels of the  $S_R^3$  potential,  $\mathcal{V}(r\sqrt{\tilde{\kappa}}, \tilde{\kappa})$ , in eq. (33), taken as the quark-diquark confinement potential. The potential parameters are those from eq. (39). Double bars represent parity dyads, single bars the unpaired states of maximum spin. The notion  $L_{2I,2J}(-)$  has been used for resonances “missing” from a level. The model predicts two more levels of maximal spins  $J^\pi = 5/2^+$ , and  $J^\pi = 9/2^+$ , respectively, which are completely “missing”. In order not to overload the figure with notations, the names of the resonances belonging to them have been suppressed. The predicted energy at rest (equal to the mass) of each level is given to its most right.

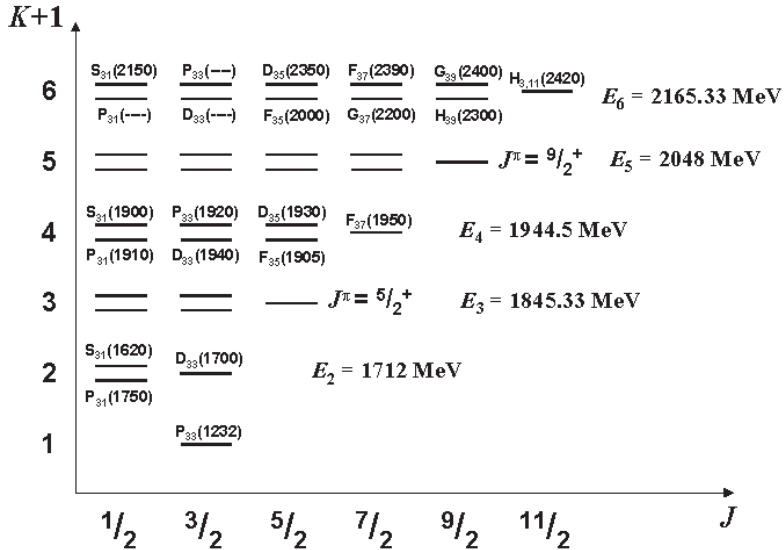


Figure 3: Assignment of the reported  $\Delta(1232)$  excitations to the  $K$  levels of the  $S_R^3$  potential  $\mathcal{V}(r\sqrt{\tilde{\kappa}}, \tilde{\kappa})$  in eq. (33), taken as the quark-diquark confinement potential. The potential parameters are those from eq. (39) with exception of the  $d$  value taken here as  $d = 3$  fm. Other notations same as in Fig. 2.

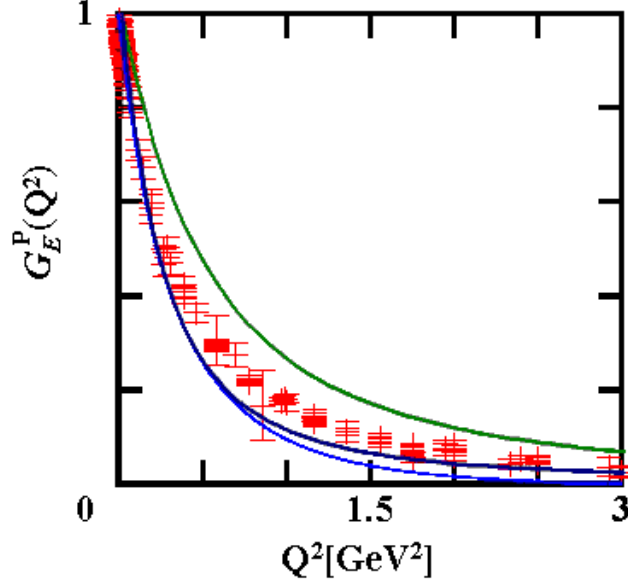


Figure 4: The electric charge form factor of the proton calculated for various curvature parameters. The upper curve corresponds to the curvature as fitted to the nucleon spectrum, the curvature leading to the middle curve has been fitted to the experimental value of the mean square of the charge radius (see Table 1). The lowest curve follows from a Bethe-Salpeter calculation based upon an instanton induced two-body potential and has been presented in ref. [55]. Data compilation taken from [55].

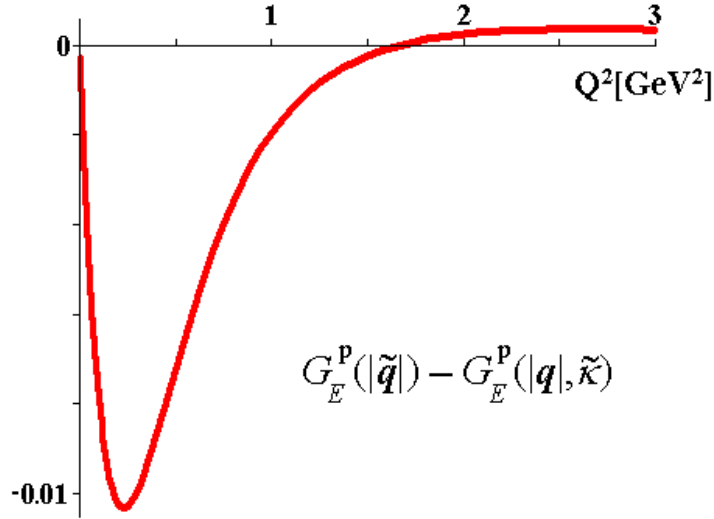


Figure 5: Difference between the electric charge form factor,  $G_E^p(|\mathbf{q}|, \tilde{\kappa})$ , calculated in  $E_4$ , with  $\tilde{\kappa} = 1/d^2$ ,  $d = 2.31$  fm, and  $G_E^p(|\tilde{\mathbf{q}}|)$  with  $|\tilde{\mathbf{q}}| \equiv |\mathbf{q}|d$  calculated in [17] in ordinary three space in closed form for the same  $d$  value. On the figure the form factors have been plotted as functions of  $Q^2 = -\mathbf{q}^2 = |\mathbf{q}|^2$ . The insignificance of this difference illustrates consistency of the three-dimensional Fourier-transform with the small  $\chi$  angle approximation to the four-dimensional Fourier transform in the  $D(r, \kappa) = r\pi$  gauge.

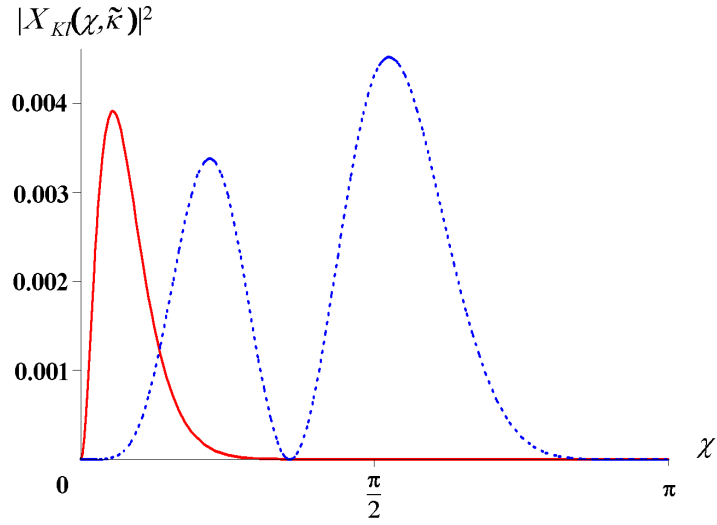


Figure 6: Charge density profiles in the ground state (solid line), and the  $K = 3, l = 2$  excitation (dashed line), corresponding to the first  $F_{1,5}$  resonance. The wave function have been taken unnormalized. It is visible that while the former damps the small  $\chi$  angle contributions from the four dimensional plane wave, the latter captures a significant amount of them which enables it to distinguish flat from curved spaces.

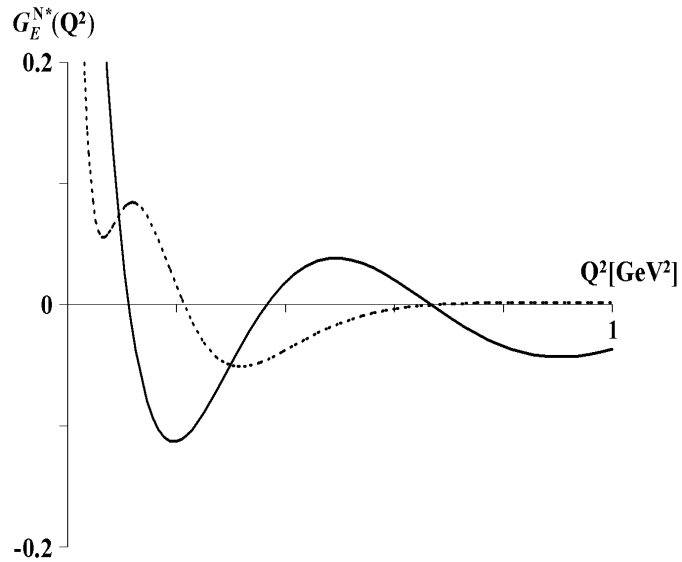


Figure 7: Electric charge form factor of the  $K = 3, l = 2$  resonance from plane space (dashed line) versus the  $S_R^3$  one (solid line). It is visible that in the vicinity of  $Q^2 = 1 \text{ GeV}^2$ , the curved space predicts a non-zero form factor versus a vanishing one following from flat space.